



Assessment of Soil Gas Radon and Exhalation Studies in Lower Himalayan Region of Jammu and Kashmir State, India

SUMIT SHARMA,^{1,2} AJAY KUMAR,¹  ROHIT MEHRA,² and ROSALINE MISHRA³

Abstract—In the present work, the soil gas radon survey has been carried out for locating the trend of soil radon in the foothills of Siwalik which is covered with lithology of Pliocene unconsolidated deposits. Soil gas radon concentration and mass exhalation rate have been studied in natural soil samples of Udhampur district, Jammu and Kashmir, India using active measurement technique RAD7 and smart RnDuo monitor. The sampling measurements were chosen according to suitability of the area. Few of the locations are near the Main Boundary Thrust (MBT) and tectonically active lineaments, having reasonably high concentration of soil gas radon. The soil gas radon concentration in 15 locations of studied area has been measured at different depths (30, 45 and 60 cm) and the overall soil gas concentration was found to vary from 0.14 to 61.01 kBq m⁻³, respectively. This large variation in radon content might be due to radioactive nature of the bedrocks present in different geological structure. Soil pore diffusion model have been used to observe the relation between experimentally and theoretically determined soil gas radon concentrations in the studied region.

Key words: RAD7, smart RnDuo monitor, geology, exhalation rate, soil gas radon.

1. Introduction

Noble gases are chemically inert; therefore, these are used in many fields for a number of applications. Spatial variations of these gases, primarily radon and helium, is useful in many studies such as geophysical tracer for locating hidden faults/thrust, in metrology, medicine, water research and in seismic monitoring activities (Banwell and Parizek 1988; Walia et al.

2006; Fu et al. 2005; Fleischer et al. 1975). Radon has three isotopes; ²²²Rn (radon), ²²⁰Rn (thoron) and ²¹⁹Rn (actinon). Radon is the short-lived decay product of uranium (²³⁸U) series with a half-life of 3.82 days. Thoron is a decay product of thorium (²³²Th) series with a relatively short half-life (55 s) that makes it useful in very fast soil gas transport and in thorium-rich soil. Due to short half-life of actinon (4 s), it is neglected in geochemical exploration. In past, many investigators have made efforts to find the relationship between these gases and seismically active areas (Kumar et al. 2013).

Natural background radiations have terrestrial and extra-terrestrial source of origin and general population is continuously exposed to these radiations. Extra-terrestrial radiations are cosmic radiations having subatomic particles which come from outside the earth's atmosphere (Saini and Bajwa 2017). Terrestrial sources (²³⁸U, ²³²Th and ⁴⁰K) have their own characteristic radioactivity. Uranium has a ubiquitous presence in earth crust.

The radon emanation from ground to atmosphere mainly depends upon the ²²⁶Ra content and the mineral grain size. Two main factors responsible for transportation of radon in environment are mass diffusion (it is a concentration gradient between the point of birth of radon and the atmosphere) and advection (movements caused by air pressure differentials) (UNSCEAR 1988). Radon transport is thus controlled by geophysical and geochemical parameters while exhalation is controlled by hydro-meteorological conditions (Etiopie and Martinelli 2002). Emanation coefficient also depends upon the water content and radon transport parameters in soil (Stranden et al. 1984).

¹ Department of Physics, DAV College, Amritsar, Punjab 143001, India. E-mail: ajay782@rediffmail.com

² Department of Physics, Dr. B R Ambedkar National Institute of Technology, Jalandhar, Punjab 144011, India.

³ Radiological Physics and Advisory Division, Bhabha Atomic Research Centre, Mumbai 400082, India.

The high concentration characteristics of radon over faults reflect gas migration dominated by brittle deformation both at macro- and/or microscale. Therefore, spatial patterns of soil gas radon in faulted areas appear to be suitable tools for identifying and mapping active tectonic structures (Baubron et al. 2002). A fault is a fracture or zone of fractures that separates different blocks of crust and accumulates a seismic strain subjected to large stress concentrations. The study of fault zone and its mapping is important for understanding earthquake predictions and for seismic hazard analysis (Kumar et al. 2013). Faults/cracks are the main pathway for ascending of gases and are identified by detecting high values of radon and thoron concentrations in soil (Botond et al. 2014). By knowing the position and activity of the fault, people mostly avoid building houses or any structure on the faults which would be destroyed when fault breaks the earth's surface. Soil gas radon concentration is generally high along the faults and at intersection points (Etiope and Lombardi 1995; King et al. 1996). But the presence of faults does not guarantee anomalous radon activity concentration always because the behavior of soil gas is also controlled by some other phenomena such as climate factor, moisture content and gas behavior (mobility, solubility, and reactivity) as these factors influence the transportation of radon (Ciotoli et al. 1998).

Radon and its progenies from soil, water and rocks are the main cause of radon-related problems. According to National Academy of Science 1998 BEIR Report, there are annually about 21,000 lung cancer deaths due to radon and its short-lived decay products. It is well established fact that the populace exposed to high concentration of radon and its daughter products for a long period of time suffer from pathological effects such as change in immune system, respiratory function problems and occurrence of lung cancer (USEPA 2012).

In the present investigation, the soil gas radon concentration, radon mass exhalation rate and radium (^{226}Ra) concentration measurements were carried out in tectonically active (Siwalik and Murree) region of Udhampur district of Jammu and Kashmir state, in the NW Himalayas, India. Soil gas radon concentrations were measured at various depths to find the influences of soil gas on local environment and its

togetherness (correlation coefficient) if any, have also been analyzed with radium (^{226}Ra) activity, exhalation rate and also with the geology of tectonically active areas. The main aim of this study is to evaluate the local levels of soil gas radon, creating soil gas radon map, geological information and identification of radon-prone areas in the study region and to find its variance with soil pore diffusion model.

2. Geology of the Study Area

The investigated area as shown in Fig. 1 is located in Udhampur District along MBT (Reasi Inlier). The district has varied topography. The most area of the district is covered by hills and mountains. The altitude variation in district is approximately 600–2500 m above the mean sea level. The topography of the area is rugged with high mountains and deep dissected by rivers Tawi and Ujh. The Udhampur district is divided in three litho-tectonic domains such as Siwalik, Murree and Ramban and Sincha group. The Reasi Inlier occurs in detached inliers of Jammu region and extends westwards to the oil producing potwar Basin in Northeast Pakistan. The Reasi Inlier, 40 km long and 12 km wide, is the largest inlier in this region. This comprises of reservoir quality, dark-gray dolomite, limestone with seal horizons of chert and argillites and organic-rich shale intervals. The lime stones possess vuggy, inter- and intragranular, fracture, inter- and intra-layer porosities. The shale with organic matter content of 10% has oil/gas-generating potential. Some of these carbonate and shale horizons yield Neoproterozoic microflora comparable with those reported in North African Neoproterozoic sandstones and late Proterozoic carbonates of the giant oil and gas fields of the Baikit Anticline of the Siberian Platform (Krishnan and Prasad 1970).

Upper Murree and Lower Siwalik are very well exposed north of the Kishanpur Nagrota-Mandli section of Udhampur-Dhar road. The geological sequence of the rock formations in the area is given in Table 1. The rocks exposed immediately above the Middle Siwalik with a thrust contact from Kishanpur Nagrota to Mandli are Upper Murree, because they show sedimentological characters (Zircon types

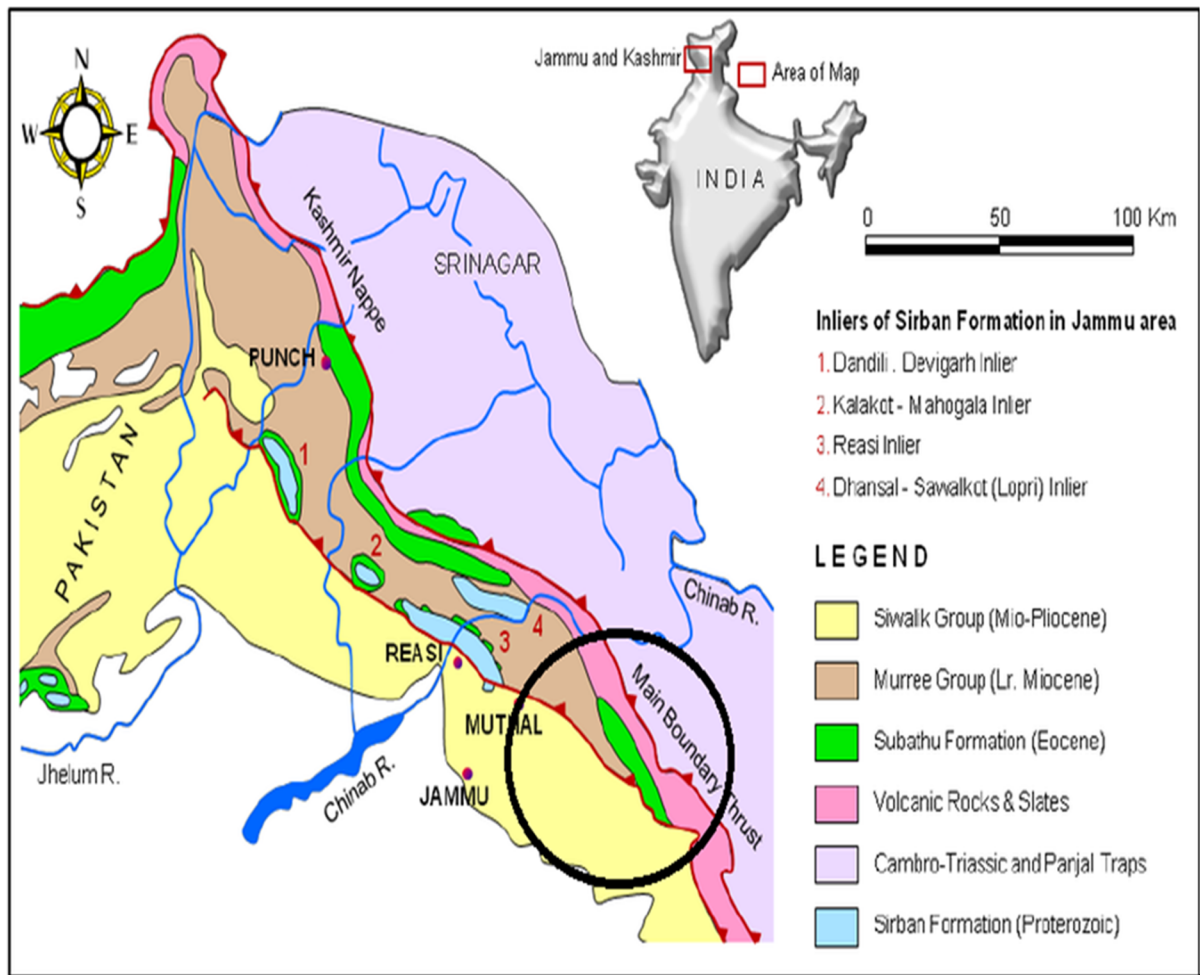


Figure 1
Regional geological map of Siwalik and Murree group with Sirban formation and Reasi inlier

Table 1

Different formation in the study region and their descriptions

Formations	Description
Middle Shiwalik	Grey, medium grained sandstones. With subordinate buff, ash grey and purplish clays.
Lower Shiwalik	Kamlial stage Brown, red and orange clays with grey purple, fine grained sandstones
	Chinji stage Hard, fine grained, grey, purple greenish grey Sandstone, clays and siltstones.
Upper Murree	Hard, fine grained, purple, greenish grey, and grey sandstones, clays and siltstones.

and grain size studies) very closely resembling the undoubted Upper Murree exposed north of the Main Boundary fault in the Udhampur area. These Upper Murree are conformably succeeded by Kamlials; and both these units exhibit similar lithological characters. The Kamlials pass conformably into the Chinji stage and the latter is distinguished by the dominance of clay in comparison to sandstones. The beginning of Chinji stage is also marked by a change in the grain size of sandstones and incoming of bright red clays. The entire area is a major anticline and the studied part forms its northern faulted limb (Sahni and Mathur 1964). The Siwalik Group of Jammu division is mostly exposed in outcrops that occupy an intermediate position between the type sections on the west and Siwalik Hills of Chandpur in east having type localities Pinjor and Boulder Conglomerate. Various lithostratigraphic units starting from Chinji Formation to Boulder Conglomerate Formation have been delineated in this area (Pascoe 1964). The Upper Siwalik subgroup of rocks of Jammu region has been divided into Parmandal Sandstone, Nagrota Formation, and Boulder Conglomerate (Ranga et al. 1988). The Siwalik Group is also divided into Mansar Formation (Lower Siwalik Subgroup); Dewal Formation (= Nagri), Mohargarh Formation (= Dhok Pathan) (Middle Siwalik Subgroup); and Uttarbehani Formation and Dughor Formation (= Boulder Conglomerate) (Upper Siwalik Subgroup) (Gupta and Verma 1988).

3. Experimental Detail

3.1. Sampling

In the present study, sampling is done along Kishanpur-Mandli thrust (MBT) and other various transverse lineaments which also act as small thrusts/faults (Madun thrust) as shown in Fig. 2. The sampling interval is limited due to tough terrain, improper site locations and other practical/field problems. For this, one hole was drilled on each location down to the bedrock surface. Soil gas radon concentration has been carried out in couple of days in the month of May 2017 covering an area about 45 km² with 15 sampling sites within the urban and

rural area of Udhampur district. These representative sampling sites were also taken for the measurement of mass exhalation rate in natural soil. Soil samples were collected from the each sampling site at the depth of 10–20 cm from the soil surface for exhalation study. Radon gas in soil and mass exhalation rate were measured at the sampling site by active technique RAD7 and Smart RnDuo monitor.

3.2. Measurement of Radon Gas Concentration in Soil

RAD7 of Durrige Company, USA, has been utilized for the monitoring of soil gas radon activity concentration. A hollow steel probe of diameter 3 and 10 cm in length with sharp pointed tool for piercing the hole is at the end of the probe for drilling into the soil. It also prevents the soil from blocking the probe. This probe is immersed into the ground at different depths with the gentle stock of hammer and not possible to inert the probe below the suggested depth of 1 m (Barnet et al. 2008). Probe is connected to the RAD7 through the drierite in the closed-loop circuit as shown in Fig. 3. At the time of measurement, the detector operates in external relative humidity ranging from 0 to 95% and the internal relative humidity 0–10% with low detection limit of 4 Bq m⁻³ and an upper detection limit of 400 kBq m⁻³. Larger the relative humidity, lesser is the detection efficiency of the RAD7 detector (Kumar et al. 2014). In many instruments and techniques, radon and thoron interfere with each other and it is impossible to measure one accurately in the existence of other. But, RAD7 is much less susceptible to radon thoron interference due to its ability to distinguish the isotopes by their alpha energies. Briefly, RAD7 starts working when air is circulating from the ground through a membrane filter which hold airborne particulate issue containing radon progeny and through desiccant to anticipate radon artifacts amid estimations. This purified air enters the RAD7 measuring chamber where radon gas is detected through the decay products of its daughters (²¹⁸Po) produced inside the chamber. During sampling, RAD7 is operated in sniff mode with grab sampling. Since, radon and its progeny (²¹⁸Po) has taken the 15 min to attain the secular equilibrium and a solitary measurement must

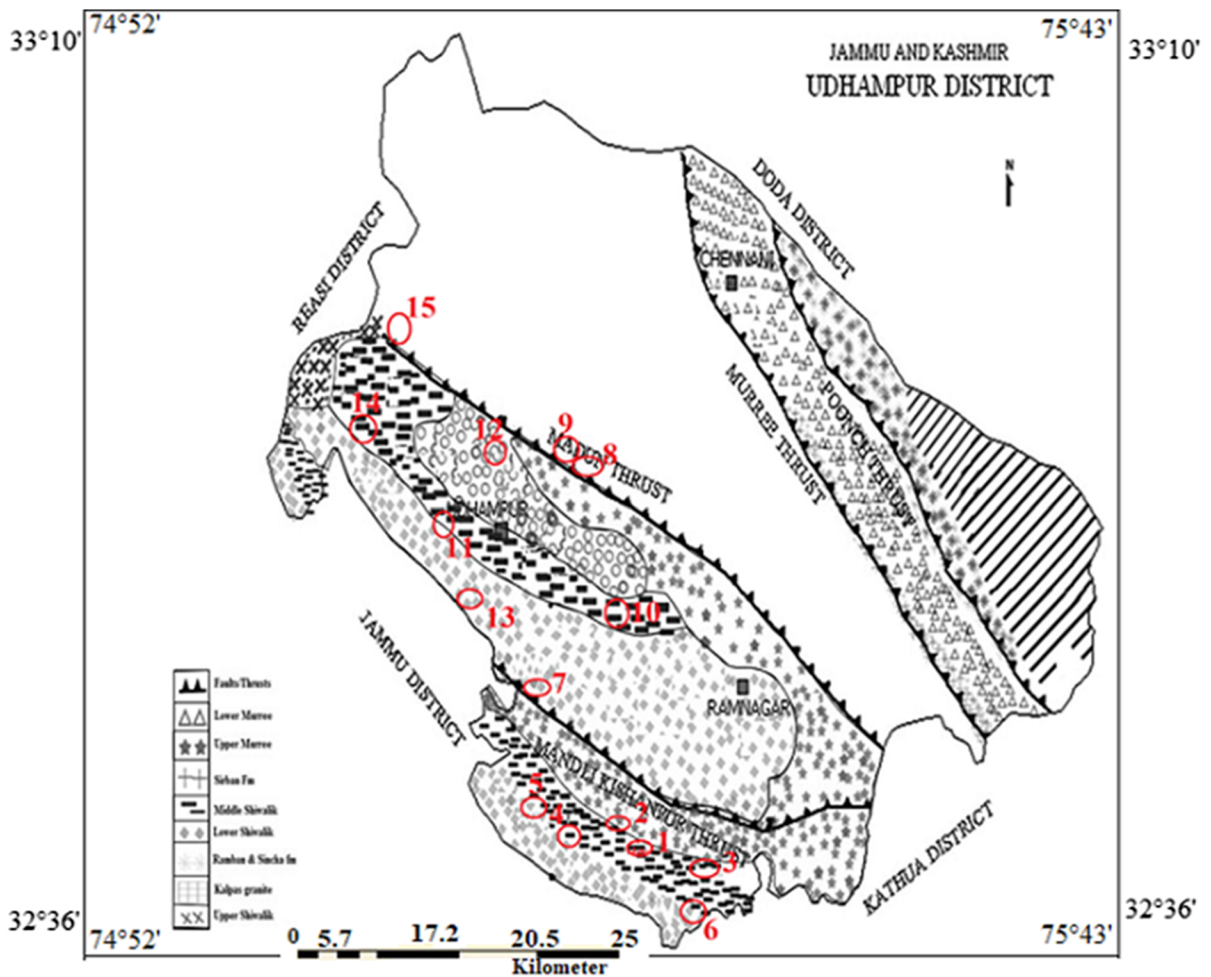


Figure 2
Surveyed locations in the study area

have an average duration of 25–30 min with every readings taken 5 min, data is received in the form of bar charts and cumulative spectra of the sample through printer (Cinelli et al. 2014).

3.3. Mass Exhalation Rate

Radon mass exhalation rate in soil samples were measured using advanced smart RnDuo Monitor (SRM), manufactured and calibrated at BARC (Gaware et al. 2011). The collected soil samples were first dried to make it moisture free and then put in the exhalation chamber (stainless steel) of inner height 8 cm and radius 4.5 cm. Exhalation chamber is connected to SRM through diffusion mode as

shown in Fig. 4. Alpha particles emitted from sampled radon/thoron and its decay products are detected in the detector volume (153 cc) by scintillation with ZnS(Ag). The alpha counts obtained from each interval (1 h) are converted into ^{222}Rn activity concentration (Bq m^{-3}) using an algorithm implemented in the micro-controller. In this technique, there is no interference of thoron and its decay products in concentration values and leakage of gas like sealed canister technique (Gaware et al. 2011). The monitor has a sensitivity factor of 1.2 counts $\text{h}^{-1} \text{Bq m}^{-3}$ with detection range of 8 Bq m^{-3} to 10 mBq m^{-3} . The growth of radon mass exhalation in chamber has been carried out for each sample till the saturation of radon concentration is obtained and

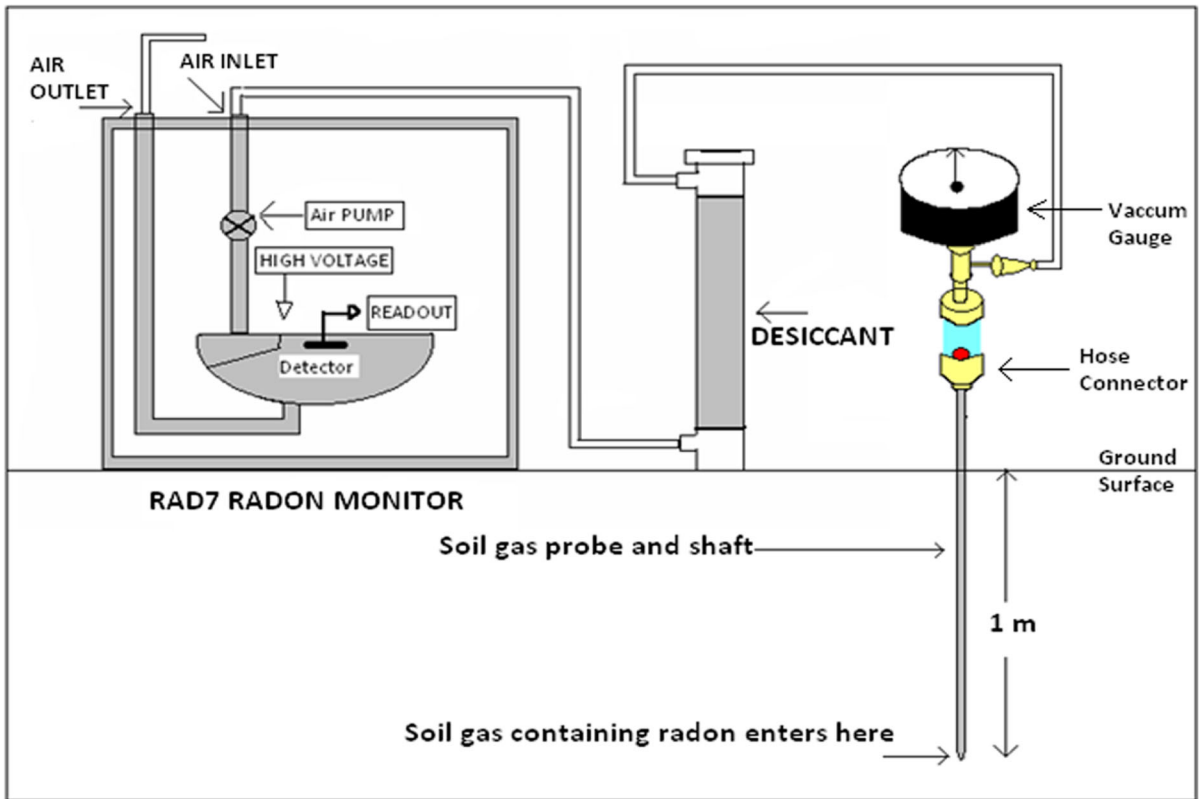


Figure 3
Schematic diagram of the RAD-7 soil gas setup

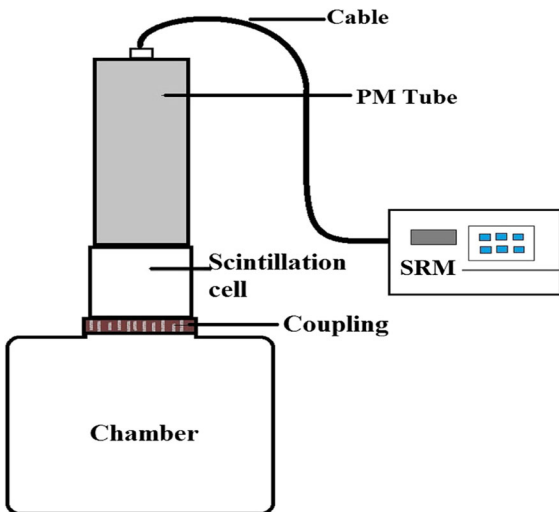


Figure 4
Schematic diagram of radon mass exhalation setup

radon mass exhalation rate (J_m) is estimated using the least square fitting method for radon concentration $C(R)$ at time (t) (Sahoo et al. 2007).

$$C(t) = \frac{J_m M}{\lambda_e V} (1 - e^{-\lambda_e t}) + C_0 e^{-\lambda_e t},$$

where J_m represents the radon mass exhalation rate in ($\text{Bq kg}^{-1} \text{h}^{-1}$). M is the mass of soil sample (kg), V is the residual volume of the chamber and the volume of the scintillation cell (m^3), λ_e is the effective decay constant which is the sum of ^{222}Rn decay constant and any chamber leakage decay rate if exists, and C_0 is the initial radon concentration in chamber.

4. Theoretical Evaluation of Soil Gas

Theoretical estimation of soil gas radon concentration is also estimated using the soil pore diffusion model proposed by Nero (1988). This model is

Table 2

Soil gas radon and mass exhalation rate in 15 locations of Udhampur district, Jammu and Kashmir State, India

Sr. no.	Village name	GPS		Humidity (%)	Soil gas radon (kBq m ⁻³)			Mass exhalation rate (mBq Kg ⁻¹ h ⁻¹)
		Latitude	Longitude		30 cm	45 cm	60 cm	
1.	Bilaspur	32°41.158'	75°15.426'	22	0.15 ± 0.03	9.03 ± 0.07	2.4 ± 0.12	29.57 ± 1.02
2.	Chugwan	32°41.562'	75°14.718'	18	0.18 ± 0.04	19.25 ± 0.83	4.32 ± 0.2	36.31 ± 1.06
3.	Puthwar	32°41.004'	75°17.602'	17	0.89 ± 0.06	21.0 ± 1.87	6.59 ± 0.16	17.96 ± 0.64
4.	Banara	32°41.625'	75°13.088'	19	2.39 ± 0.17	39.01 ± 2.69	7.34 ± 0.19	24.54 ± 0.62
5.	Baryalta	32°42.572'	75°10.911'	16	5.83 ± 0.15	61.02 ± 0.71	7.6 ± 0.16	13.04 ± 0.67
6.	Omara	32°38.612'	75°18.057'	12	0.14 ± 0.04	8.79 ± 0.09	1.29 ± 0.06	20.04 ± 0.59
7.	Darsoo	32°47.941'	75°08.415'	15	0.71 ± 0.04	10.25 ± 0.43	1.42 ± 0.13	27.24 ± 0.91
8.	Rount	32°56.303'	75°07.977'	19	0.41 ± 0.14	20 ± 1.7	2.52 ± 0.13	35.64 ± 2.01
9.	Gangera	32°56.383'	75°08.422'	21	0.62 ± 0.18	26.5 ± 1.12	4.27 ± 0.24	25.37 ± 0.76
10.	Jaganoo	32°52.261'	75°08.798'	24	0.84 ± 0.07	11.56 ± 1.46	1.54 ± 0.4	15.57 ± 0.72
11.	Jib	32°55.129'	75°03.291'	17	0.36 ± 0.10	1.46 ± 0.21	0.84 ± 0.06	21.68 ± 1.25
12.	Jakhar	32°56.240'	75°07.187'	18	0.19 ± 0.02	1.53 ± 0.43	0.96 ± 0.24	30.31 ± 0.78
13.	Seen	32°54.341'	75°02.480'	18	4.56 ± 0.29	22.01 ± 1.39	7.36 ± 0.86	23.98 ± 1.82
14.	Tikri	32°56.885'	74°58.956'	21	1.36 ± 0.25	19 ± 1.36	2.53 ± 0.48	21.51 ± 1.15
15.	Muttal	32°58.984'	75°01.874'	18	1.96 ± 0.35	26.01 ± 1.52	6.46 ± 0.19	21.26 ± 0.64
	Min				0.14	1.46	0.84	13.04
	Max				5.84	61.01	7.59	36.31
	Average				1.37	19.76	3.82	24.25
	S.D.				1.65	14.66	2.49	6.49
	G.M.				0.71	13.73	2.95	23.38

applicable to both diffusive and advective transport of radon. It is the hypothetical result obtained from one-dimensional steady-state transport of radon from homogenous isotropic soil. In one-dimensional transport of soil radon, the model gives the soil radon concentrations at different depths as shown below:

$$C(Z) \approx (1 - e^{-\sqrt{\lambda_{Rn} D_e} Z}) c(-\infty),$$

where C is the radon concentration in pores (Bq m⁻³), D_e is effective diffusion coefficient of radon in soil (m² s⁻¹), λ_{Rn} the radon decay constant in second.

$$c(-\infty) = \frac{G}{\lambda_{Rn}},$$

where G is radon generation rate in soil pores (Bq m⁻² s⁻¹) and measured as:

$$G = A_{Ra} \times \rho \times f \times \lambda_{Rn} \times \left(\frac{1 - \varepsilon}{\varepsilon} \right),$$

where A_{Ra} is the radium (²²⁶Ra) activity concentration (Bq kg⁻¹), ρ is bulk density of the material (kg m⁻³), f is the emanation factor, ratio of the radon concentration emanation from air-filled pores to the

total radon production from the material. Some important parameters were set equal to (Nero 1988):

$$\varepsilon = 0.434;$$

$$D_e = 2 \times 10^{-6} \text{ m}^2 \text{ s}^{-1} \text{ for normal soil};$$

$$5 \times 10^{-6} \text{ m}^2 \text{ s}^{-1} \text{ for dry soil};$$

$$2 \times 10^{-7} \text{ m}^2 \text{ s}^{-1} \text{ for wet soil, respectively.}$$

5. Results and Discussion

The results obtained from the measurement of soil gas radon activity concentration at different depths of Udhampur district has been tabulated in Table 2. At a depth of 30 cm, the soil gas radon concentration has been observed to be varying from 0.14 to 5.84 kBq m⁻³ with an average value of 1.37 ± 1.62 kBq m⁻³. At 45 cm, the minimum and maximum soil gas concentrations have been found to be 1.46 and 61.01 kBq m⁻³. The average activity concentration of soil gas at 45 cm was 19.76 ± 15.66 kBq m⁻³. At 60 cm, the soil gas

concentration varied from 0.84 to 7.59 kBq m⁻³ with an average of 3.82 ± 2.58 kBq m⁻³. The overall maximum value of soil gas radon concentration was found in Baryalta (61.01 kBq m⁻³) which is near the MBT and minimum value was found in Omara (0.14 kBq m⁻³). Locations along Main Boundary Thrust (MBT) i.e., Kishanpur-Mandli thrust (Baryalta, Banara, Chugwan and Puthwar) and near the local thrust, i.e., Madun thrust (Rount, Gangera, and Mittal) have comparatively higher soil gas radon concentrations than the other locations.

A scattered plot of soil gas radon concentrations is plotted in Fig. 5. The plot shows the variation of soil radon concentration at different depths (30, 45 and 60 cm) at each sampling site. From the obtained results, it is observed that as we move from 30 to 45 cm down the earth, soil gas radon concentration increases. At the depth of 45 cm, the maximum soil gas radon concentration has been obtained. After that, as we move down from 45 to 60 cm, the observed concentration of soil gas radon decreases. Comparatively less gas concentration at 60 cm might be due to underlying bedrocks, compact packing of sandstones/bedrocks and soil permeability at that particular position, resulting poor migration of radon gas. The results of this study agree with the results of reported by Tareen et al. (2016) for very high hazard area of Muzaffarabad, Pakistan and Kaur et al. (2018) for Siwalik Himalayas, Jammu and Kashmir. Soil gas radon concentration in Udhampur district has also been compared with the radon concentration in water samples reported in our published papers (Kumar et al. 2017). For instance, as we observe the radon level at Baryalta location, it is found maximum in soil gas as well as in water as reported in the above-mentioned paper. It is also evident from the correlation studies that the values of soil gas radon concentrations are in close agreement with that of radon in water (Fig. 6a). The high values of soil gas and radon concentration in water samples were found at Baryalta and Banara locations. These two locations are at the share zones of the two geological formations as shown in the map which act as thrust and small lineament and migrate radon gas. Soil gas radon concentration has also been compared with the radon concentration in indoor environment of Udhampur district reported in published data (Sharma

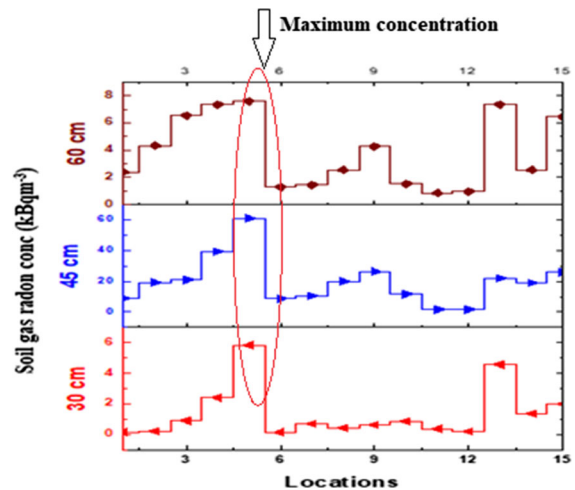


Figure 5
Variation of soil gas radon at different depths

et al. 2018). Same conclusion has also been drawn from this correlation study that, where the soil gas radon is high, the indoor radon level is also high. Therefore, positive correlation between soil gas and indoor radon level indicates that soil is the main cause of increasing radon level in the dwellings (Fig. 6b).

Figure 5 shows that the soil gas radon concentration in the environments of Siwalik formation are higher than that of the Murree formation. Maximum activity concentrations were obtained at Baryalta location at each depth, in this formation as marked in Fig. 5. The main sources of soil gas radon are uranium and radium and their distribution, permeability, moisture content and porosity of the soil. The principal sources of uranium and radium in soil are minerals (salts), iron oxide coating on rocks, soil grains and organic materials in soil and sediments, phosphate and carbonate complexes (Devoto 1984). The low value of soil gas concentration in Murree region of Pakistan was also reported by Ali et al. (2010). These lithological units may potentially be the cause of soil gas radon concentrations in these areas. This is also relied upon the observed concentration in two distinct geochemical (Siwalik and Murree) matrices with different uranium–radium concentration levels: Soil gas radon concentration in these three different sets will reflect both parent lithology portrayed by Kumar et al. (2017).

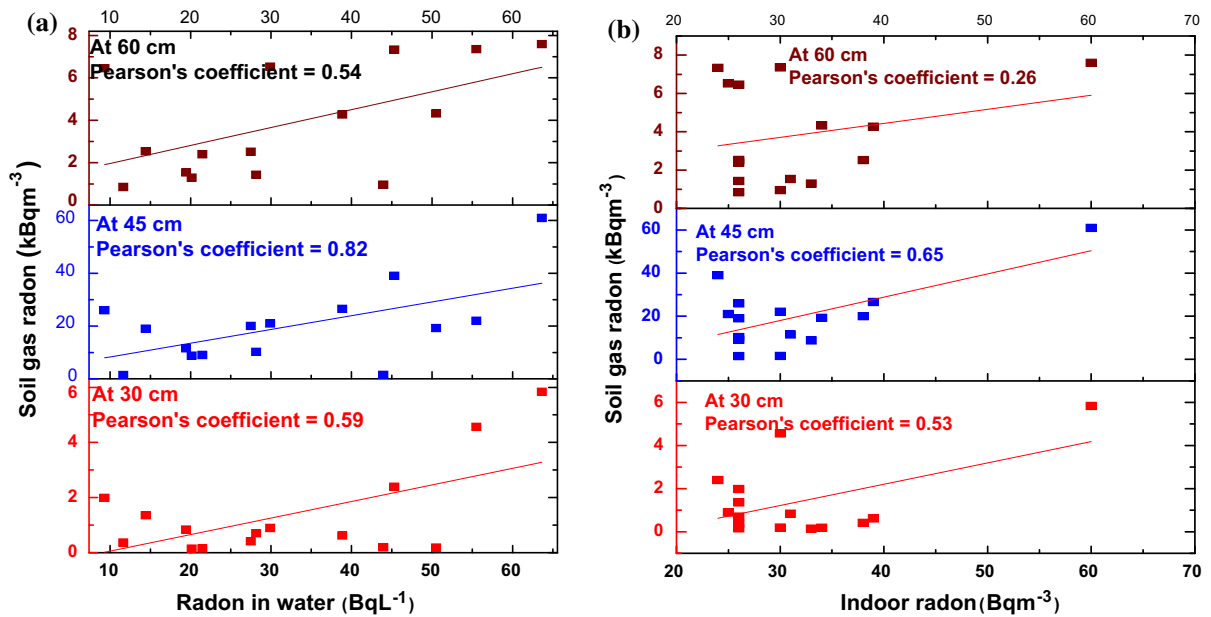


Figure 6

a Correlation between dissolved radon (Bq L^{-1}) vs. soil gas radon concentration (kBq m^{-3}). **b** Correlation between indoor radon (Bq m^{-3}) vs. soil gas radon (kBq m^{-3})

Table 3

Comparison of soil gas radon concentration with reported values by other investigators

Regions	Range (KBq m^{-3})	References
Islamabad, Pakistan	17.34–72.52	Ali et al. (2010)
Murree, Pakistan	0.61–3.89	Ali et al. (2010)
Southern Punjab, Pakistan	0.42–3.56	Mujahid et al. (2010)
Budhakedar, Tehri Garhwal, India	1.10–31.80	Prasad et al. (2008)
Hamirpur district, HP	0.03–2.28	Mehra and Bala (2013)
Garhwal Himalaya, India	0.01–2.33	Bourai et al. (2013)
Upper Siwaliks, India	11.50–78.47	Singh et al. (2010)
Amritsar, Punjab	14.4	Kumar et al. (2012)
Malwa belt, Punjab, India	1.90–16.40	Kumar et al. (2011)
Tusham ring, Haryana, India	42.80–71.50	Bajwa et al. (2010)
Kangra district, HP, India	1.10–82.20	Singh et al. (2006)
Siwalik region of Dharamshala	13.6–70.2	Kumar et al. (2014)
Dharamshala sandstones	13.2–66.2	Kumar et al. (2014)
Alluvium of Dharamshala	18.8–110.8	Kumar et al. (2014)
Udhampur, J&K, India	1.46–61.02	Present study

Table 3 shows a comparison of soil gas data collected from some locations of Udhampur district having regional geology with other locations from

national and international places which are available in the literature. The overall result of soil gas radon concentration ($0.14\text{--}61.02 \text{ kBq m}^{-3}$) obtained in present study is comparatively lower than that in Islamabad of Pakistan (Ali et al. 2010), Upper Siwalik (Singh et al. 2010), Tusham ring, Haryana (Bajwa et al. 2010), Kangra region of Himachal Pradesh (Singh et al. 2006), Alluvium of Dharamshala (Kumar et al. 2014) but higher than that in Murree region of Pakistan (Ali et al. 2010), Southern Punjab of Pakistan (Mujahid et al. 2010), Budhakedar of Tehri Garhwal (Prasad et al. 2008), Harmirpur of Himachal Pradesh (Mehra and Bala 2013), Malwa belt of Punjab (Kumar et al. 2011) and Garhwal Himalayas (Bourai et al. 2013). The high value of soil gas radon concentration in Islamabad region of Pakistan is due to the presence of different geographical formations such as Hangu, Lackhart, Chichali, Lumshiwal and Samana Suk formations (Ali et al. 2010) while in Upper Siwalik, it is due to the presence of active fault (Singh et al. 2010). In Tusham ring of Haryana, it is due to the presence of granite rocks (Bajwa et al. 2010) while in Kangra, it is due to the presence of transverse Dehar lineament which is tectonically active (Singh et al. 2006). Alluvium

Table 4

*Statistical distribution of sampled soil gas radon concentration at different depths using independent *t* test*

Depth (in cm)	Frequency (<i>N</i>)	Mean (m) (kBq m ⁻³)	Standard deviation (σ)	Standard mean error	95% confidence interval of the difference	
					Lower	Upper
30	15	1.37	1.71	0.44	0.43	2.32
45	15	19.7	15.17	3.92	11.36	28.16
60	15	3.82	2.58	0.67	2.39	5.25

geological formation of Dharamshala has high soil gas concentration due to high porosity of the soil (Kumar et al. 2014) and having the high activity concentrations than the other formations of Dharamshala.

The findings of the present study seems to be in good agreement with the data reported by Kumar et al. (2012, 2014) which shows that the sediments which were derived from Siwalik Himalayas of Amritsar, Punjab and Siwalik formations and sandstones of Dharamshala, Himachal Pradesh have comparable soil gas radon concentration with that of the studied area. The similarity observed in reported and obtained data of soil gas radon concentration of Udhampur district and Dharamshala region as previously mentioned is due to the fact that both the regions have the same geology. This may also be due to the compact packing of the sandstones resulting in poor migration conditions of soil gas radon from deep-seated earth (Kumar et al. 2014). While the Amritsar lie in zone IV of seismic zoning map of India. The seismicity of the Amritsar is because of its closeness to the seismically active areas; Kangra and Hindu Kush areas of NW Himalayas. This may be due to the presence of active faults in NW Himalayas (Kumar et al. 2012).

Independent *T* test has been applied on soil gas radon concentrations measured in two different geological regions (Siwalik and Murree) of Udhampur district, Jammu and Kashmir. The statistical parameters of three different sets are reported in Table 4. Calculated 95% confidence intervals of soil radon at different depths (30, 45 and 60 cm) were found to be 0.43–2.32 kBq m⁻³, 11.36–28.16 kBq m⁻³ and 2.39–5.25 kBq m⁻³, respectively. The standard mean error shows the difference between the expected and observed data of the soil radon. The hypothetical

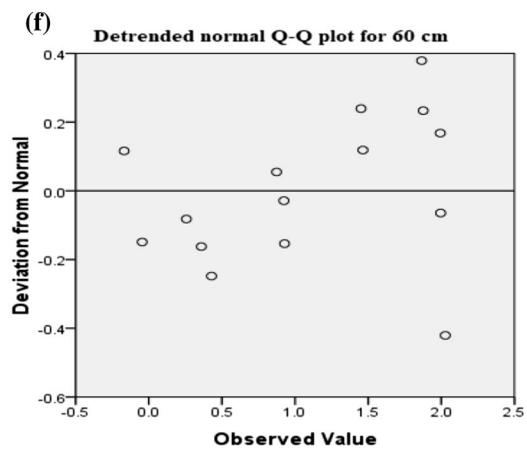
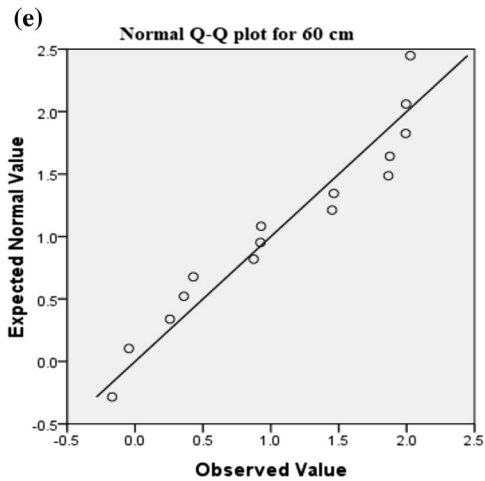
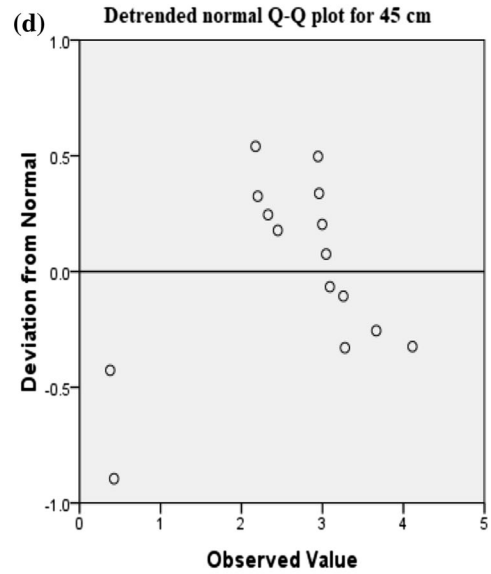
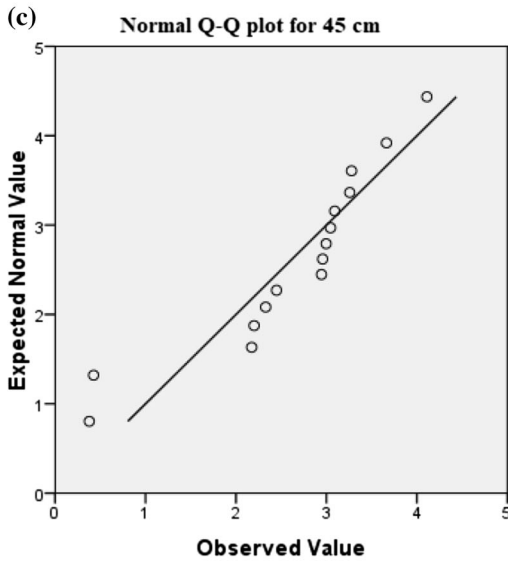
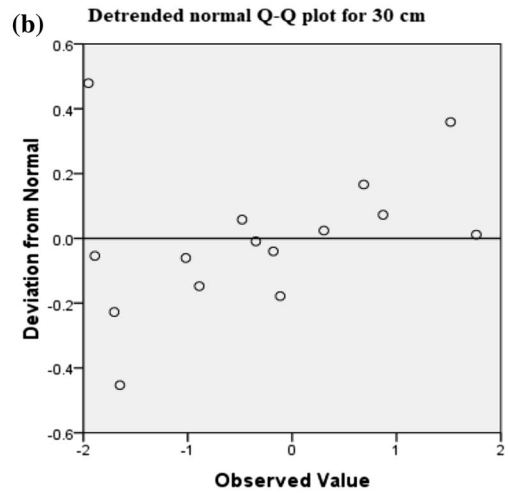
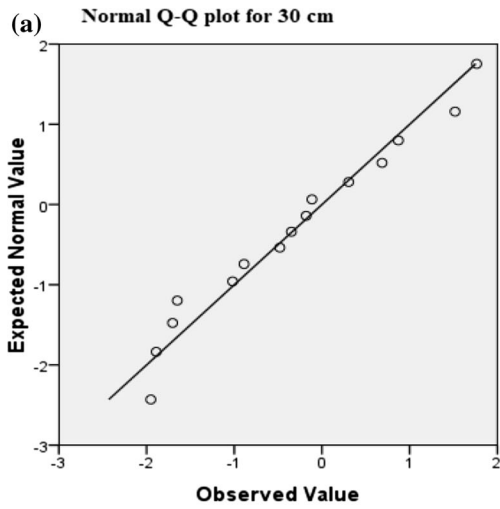
Figure 7

On the left side (figure a, c and e) are normal quantile–quantile plots for soil gas radon activity concentrations (kBq m⁻³) measured at different depths whereas on the right side (b, d and f) is Detrended Normal Quantile–Quantile Plots

normality and log normality was verified for each depth using the Q–Q plot (Fig. 7). After the *t* test, the normal Q–Q plot (Fig. 7a, c, e) compares the observed quantiles of the data (depicted as circles) with the quantiles that we would expect to see if the data is normally distributed (depicted in solid line). In a Q–Q plot, you should look for points that stray far from the line of expected values, as well as trends in the observed values. The Detrended Normal Q–Q Plot (Fig. 7b, d, f) also shows the same information as the Normal Q–Q Plot, but in a different manner. In the Detrended Plot, the horizontal line at the origin represents the quantiles that we would expect to see if the data were normal and the dots represent the magnitude and direction of deviation in the observed quantiles. Each dot is calculated by subtracting the expected quantile from the observed quantile. (This implies that if a dot is below the trend line on the Normal Q–Q plot, it will appear above the trend line on the Detrended Normal Q–Q plot, because observed-expected > 0). On the basis of statistical parameters (Table 4) and Q–Q plot (Fig. 7), the three sets belonging to different depths could be approximated with normal distribution.

5.1. Mass Exhalation Rate and ²²⁶Ra Content

Radon mass exhalation rate is calculated in collected soil samples of studied area and found to vary from 13.04 ± 0.67 to 36.31 ± 1.06 mBq kg⁻¹ h⁻¹ with an average value of 24.27 ± 6.49 mBq kg⁻¹ h⁻¹



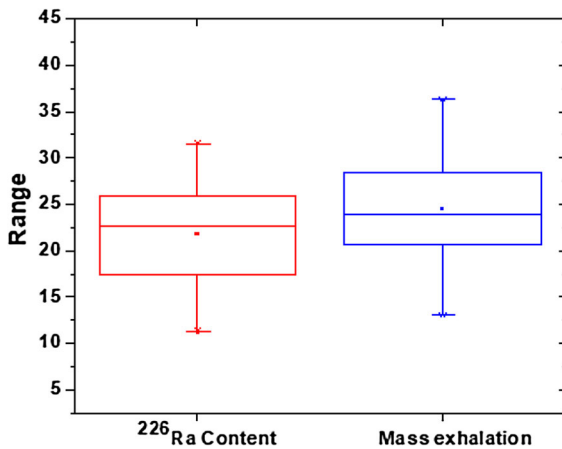


Figure 8

Box-whisker plot of ^{226}Ra content (Bq kg^{-1}) and mass exhalation rate ($\text{mBq kg}^{-1} \text{h}^{-1}$) in soil samples

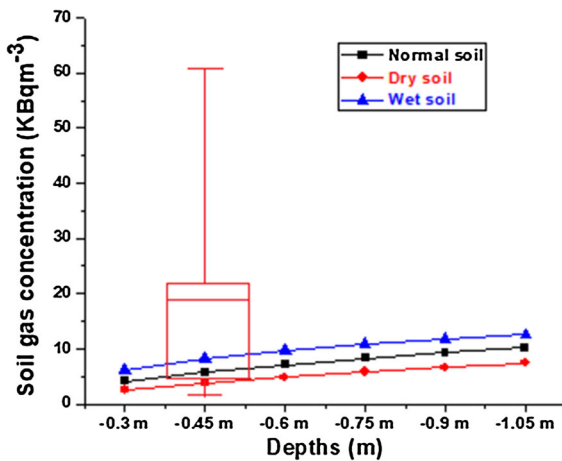


Figure 9

Theoretically calculated soil gas radon concentration for normal, dry and wet soil. Box-whisker plot represents the experimentally calculated soil radon

(Table 1). Minimum concentration of exhalation rate is $13.04 \text{ mBq kg}^{-1} \text{h}^{-1}$ for Baryalta, while the maximum exhalation rate of $36.31 \text{ mBq kg}^{-1} \text{h}^{-1}$ was measured at Chugwan. No direct correlation has been observed between soil gas and mass exhalation rate in the studied locations of Udhampur district.

The activity concentration of ^{226}Ra (A_{Ra}) in soil samples of study area was also measured by scintillation-based gamma ray spectrometer NaI(Tl). The principle and working of gamma ray spectrometer is explained elsewhere (Kumar et al. 2018; Saini and

Bajwa 2017). The observed concentration of ^{226}Ra content (A_{Ra}) varied from 11.28 to 31.52 Bq kg^{-1} with an average value of $22.34 \pm 5.54 \text{ Bq kg}^{-1}$. The reported values of ^{226}Ra content in soil samples are much lower than the world average value of 32 Bq kg^{-1} recommended by UNSCEAR (2008). From the analysis of the observed concentration, the maximum value of ^{226}Ra activity is 31.52 Bq kg^{-1} in Tikri location with mass exhalation rate of $21.51 \text{ mBq kg}^{-1} \text{h}^{-1}$ which is not too high, whereas minimum concentration of ^{226}Ra in Rount location is 11.28 Bq kg^{-1} having mass exhalation rate is $35.64 \text{ mBq kg}^{-1} \text{h}^{-1}$. Hence no correlation has been found between ^{226}Ra content and mass exhalation rate in soil samples of the study region. No correlation has been observed between soil gas radon, mass exhalation rate and ^{226}Ra content. The statistical variation of ^{226}Ra content and mass exhalation rate is shown in box whisker plot as given in Fig. 8. Moisture in the soil also affects the radon concentration, i.e., radon generation and transportation. Therefore, radon transportation is generally opposed by moisture content which blocks the soil pores with water (moisture) reducing the gas transportation from the soil. Radon atoms can diffuse through water, but if a radon particle can move around 1 m by diffusion through dry soil amid its mean expectancy, it might relocate just 1–2 cm in saturated soil during same time period (Tanner 1964). In fine grain soils having high clay content and less moisture, it is necessary to hinder radon transport from the ground because pores spaces are less and interlayer water molecules are electrostatically bound to the clay particles, so clay-rich soil holds moisture longer and tend to dry out more gradually.

5.2. Comparison Between Experimental Results and Theoretically Analyzed Soil Gas Radon Data

Soil gas radon concentration measured in Udhampur district of Jammu and Kashmir is also compared with theoretically estimated values using soil pore diffusion model given by Nero (1988). This model is helpful in providing the knowledge about soil gas concentration of any region by knowing the ^{226}Ra content and exhalation rate of soil samples of that

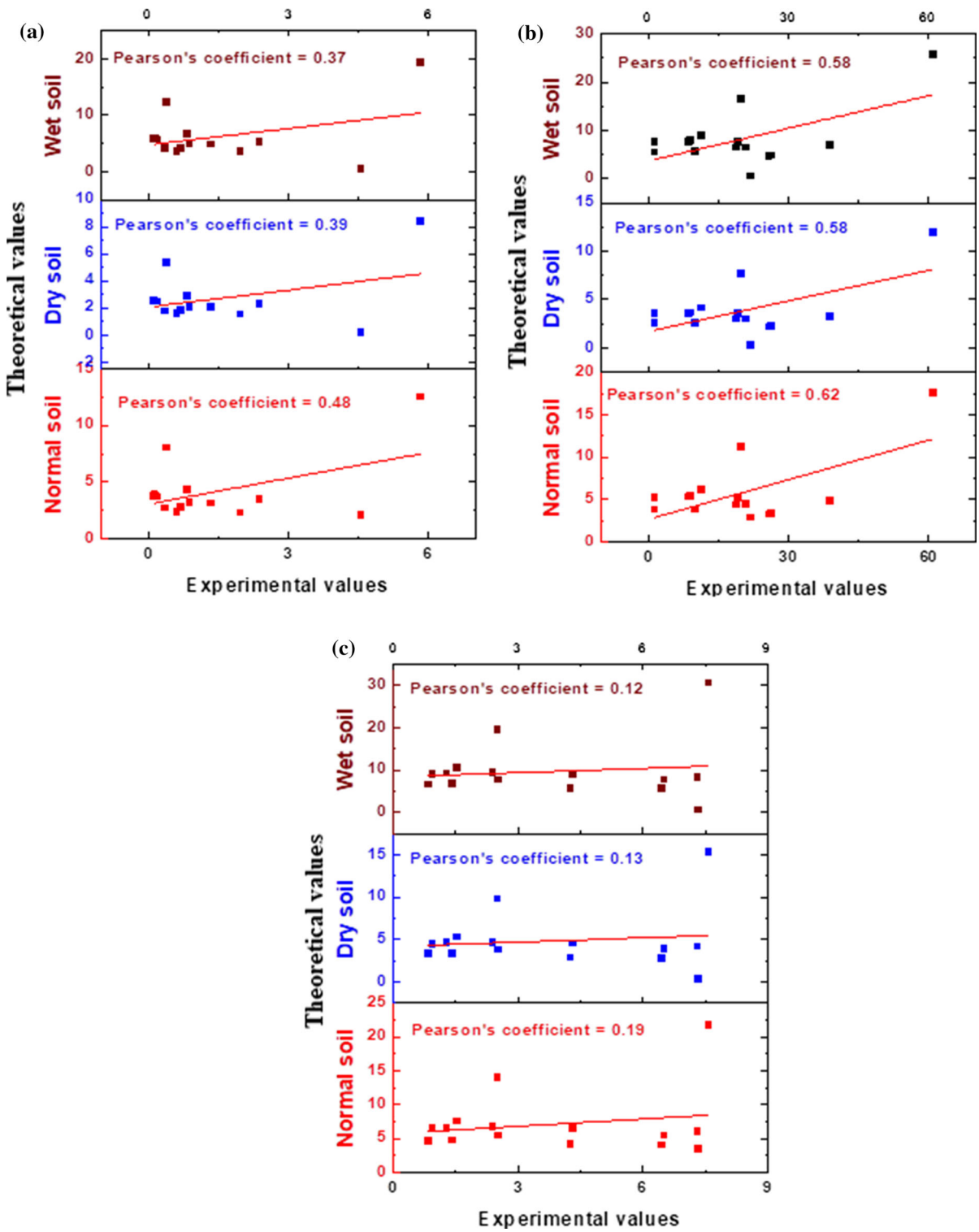


Figure 10

Correlation with experimentally observed and theoretically determined soil gas radon concentration

region. All the theoretical evaluations were carried out in research laboratory. Emanation factor in the studied locations is calculated according to Stoulus et al. (2003) and it varies from 0.11 to 0.38 with an average of 0.18. The ^{226}Ra activity concentration (A_{Ra}) was calculated for each location using Gamma ray spectrometry (NaI(Tl)) and found to vary from 39.36 to 48.39 Bq kg⁻¹. The results obtained from theoretically observed soil gas concentration profile for different soil conditions (normal, dry and wet) is reported in Fig. 9 and the box whisker plot in this figure represents the experimentally observed soil gas concentration at 45 cm. For the validation of this model, the theoretically observed soil gas radon concentration has been correlated with experimentally observed values. A positive correlation has been observed and presented in Fig. 10. It is clear from Fig. 10 that the correlation coefficient of experimentally observed and theoretically determined soil radon at particular depth (45 cm) is considerably remarkable with Pearson's coefficient of 0.62 (slope = 0.16, intercept = 2.62), 0.58 (slope = 0.10, intercept = 1.70) and 0.58 (slope = 0.22, intercept = 3.64) for normal, dry and wet soil. The concentration profile reported in these two Figs. 9 and 10 shows that theoretically determined soil gas values calculated for diffusive soil at the depth of 45 cm are in fair agreement with the experimentally measured values.

6. Conclusions

Soil gas radon measurements were carried out in Udhampur, a hilly area, having varying topography. It is mainly characterized as foothills of Siwalik and provides the initial results to investigate the sensitivity of the radon in the studied area for identifying the locations concerned with faults and hidden lineaments which is covered with unconsolidated formations. The overall soil gas radon concentration ranges from 0.14 to 61.04 kBq m⁻³. This large variation in radon concentration is due to different lithostatic units. The relatively high values of soil gas radon concentration are due to the presence of deformed structure and having higher permeability than surroundings which allows the increasing flux of

soil radon. Therefore, permeability is the main cause of controlling the variation of soil gas concentration than the geotectonic activities. The moderate level of soil gas radon concentration might be attributed due to compact nature of rocks and soil in the given bedrocks. The soil gas radon concentration results obtained in this study are consistent with the results of radon concentration in water and indoor air reported in published papers (Kumar et al. 2017; Sharma et al. 2017). No direct correlation has been observed between soil gas radon, ^{226}Ra activity and mass exhalation rate in this study because clay texture and cold climate of the studied region have impermeable soil due to high moisture content than dry soil. This type of correlation has also been reported by some investigators (Ramola and Choubey 2003; Hassan et al. 2009 and Righi and Bruzzi 2006).

The soil gas radon concentration is also measured theoretically in this study using the laboratory calculation of mass exhalation rate, emanation factor and ^{226}Ra activity in soil pore diffusion model of Nero. The theoretically obtained results of soil gas radon concentration is also consistent with experimentally observed values. Therefore, this model is too schematic to measure soil gas radon concentrations.

Acknowledgements

The authors wish to thank the Board of Research in Nuclear Science, Department of Atomic Energy (BRNS-DAE) for supporting this work financially under the major research project (sanctioned no. 2013/36/60-BRNS). The authors are also thankful to DAV College, Amritsar for their valuable cooperation during the completion of this work. We would like to thank the inhabitants of Udhampur district for their cooperation during field work.

REFERENCES

- Ali, N., Khan, E. U., Akhter, P., Khan, F., & Waheed, A. (2010). Estimation of mean annual effective dose through radon concentration in the water and indoor air of Islamabad and Murree. *Radiation Protection Dosimetry*, 141, 183–191.
- Bajwa, B. S., Singh, H., Singh, J., Singh, S., & Sonkawade, R. G. (2010). Environmental radioactivity: a case study in HHP

- granitic region of Tusham ring complex Haryana, India. *Geophysics Research Abstract*, 12, 1888. (EGU2010).
- Banwell, G. M., & Parizek, R. R. (1988). Helium-4 and radon-222 concentrations in groundwater and soil gas as indicator of fault zones of fracture concentration in unexposed rock. *Geophysical Research Letter*, 93, 355–366.
- Barnet, I., Pacherova, P., & Neznal, M. (2008). *Radon in geological environment—Czech experience Czech Geological Survey Special Papers, No. 19* (pp. 19–28). Prague: Czech Geological Survey.
- Baubron, J. C., Rigo, A., & Toutain, J. (2002). Soil–gas profile as a tool to characterize active tectonic areas: The Jault Pass example (Pyrenees, France). *Earth Planet Science Letter*, 196, 69–81.
- Botond, P., Alexandru, S., Tamás, N., Nicolae, F., Kinga, S., & Constantin, C. (2014). Soil radon and thoron activity concentrations and CO₂ flux measurements in the neogene volcanic region of the eastern carpathians (Romania). *Carpathian Journal of Earth and Environmental Sciences*, 9, 261–268.
- Bourai, A. A., Aswal, S., Dangwal, A., Rawat, M., Prasad, M., Prasad, N., et al. (2013). Measurement of radon flux and soil-gas radon concentration along the main central thrust, Garhwal Himalaya, using SRM and RAD7 detectors. *Acta Geophysica*, 61, 950–957.
- Cinelli, G., Tositti, L., Capaccioni, B., Brattich, E., & Mostacci, D. (2014). Soil gas radon assessment and development of a radon risk map in Bolsena, Central Italy. *Environmental Geochemistry and Health*. <https://doi.org/10.1007/s10653-014-9649-9>.
- Ciotoli, G., Guerra, M., Lombard, S., & Vittori, E. (1998). Soil gas survey for tracing seismogenic faults: a case study in the Fucino basin, Central Italy. *Geophysical Research*, 103, 23781–23794.
- Devoto, R. H. (1984). Uranium exploration. In B. Devivo, F. Ippolito, G. Capaldi, & P. R. Simpson (Eds.), *Uranium geochemistry, mineralogy, geology, exploration and re-sources* (pp. 101–108). London: The Institution of Mining and Metallurgy.
- Etiopo, G., & Lombardi, S. (1995). Evidence for radon transport by carrier gas through faulted clays in Italy. *Radioanalytical Nuclear Chemistry*, 193, 291–300.
- Etiopo, G., & Martinelli, G. (2002). Migration of carrier and trace gases in the geosphere: an overview. *Physics of the Earth and Planetary Interiors*, 129, 185–204.
- Fleischer, R. L., Price, P. B., & Walker, R. M. (1975). *Nuclear tracks in solids: principles and applications*. Berkeley, CA: University of California Press.
- Fu, C. C., Yang, T. F., Walia, V., & Cheng, C. H. (2005). Reconnaissance of soil gas composition over the buried fault and fracture zone in southern Taiwan. *Geochemical Journal*, 39, 427–439.
- Gaware, J. J., Sahoo, B. K., Sapra, B. K., & Mayya, Y. S. (2011). Indigenous development and networking of online radon monitors in the underground uranium mine. *Radiation Protection and Environment*, 34, 37–40.
- Gupta, S. S., & Verma, B. C. (1988). Stratigraphy and vertebrate fauna of the Siwalik, Jammu District Group, Mansar-Uttarban section, Jammu and Kashmir. *Journal of Palaeontological Society of India*, 33, 117–124.
- Hassan, N. M., Hosoda, M., Ishikawa, T., Sorimachi, A., Sahoo, S. K., Tokonami, S., et al. (2009). Radon migration process and its influence factors; review. *Health Physics*, 44, 218–231.
- Kaur, M., Kumar, A., Mehra, R., & Mishra, R. (2018). Study of radon/thoron exhalation rate, soil-gas radon concentration, and assessment of indoor radon/thoron concentration in Siwalik Himalayas of Jammu and Kashmir. *Human and Ecological Risk Assessment*. <https://doi.org/10.1080/10807039.2018.1443793>.
- King, C. Y., King, B. S., Evans, W. C., & Zhang, W. (1996). Spatial radon anomalies on active faults in California. *Applied Geochemistry*, 11, 497–510.
- Krishnan, P. V., & Prasad, R. (1970). Tectonic framework of tertiary belt of the sub Himalayas of Jammu. *Publications of the Centre of Advanced Study in Geology*, 7, 1–9.
- Kumar, A., Arora, V., Walia, V., Bajwa, B. S., Singh, S., & Yang, T. F. (2014). Study of soil gas radon variations in the tectonically active Dharamshala and Chamba regions, Himachal Pradesh, India. *Environmental Earth Sciences*, 72, 2837–2847.
- Kumar, G., Kumar, A., Walia, V., Kumar, J., Gupta, V., Yang, T. F., et al. (2013). Soil gas radon–thoron monitoring in area of north-west Himalayas, India using solid state nuclear track detectors. *Earth System Science*, 122, 1295–1301.
- Kumar, A., Sharma, S., Mehra, R., Kanwar, P., Mishra, R., & Kaur, I. (2017). Assessment of radon concentration and heavy metal contamination in groundwater of Udhampur district, Jammu and Kashmir, India. *Environmental Geochemistry and Health*, 40, 815–831.
- Kumar, S., Singh, S., Bajwa, B. S., & Sabharwal, A. D. (2011). In situ measurements of radon levels in water and soil and exhalation rate in areas of Malwa belt of Punjab (India). *Isotopes in Environment Health Studies*, 47, 446–455.
- Kumar, A., Vij, R., Sharma, S., Sarin, A., & Narang, S. (2018). Assessment of Radionuclide concentration and exhalation studies in soil of lesser Himalayas of Jammu and Kashmir. *Acta Geophysica*. <https://doi.org/10.1007/s11600-018-0119-0>.
- Kumar, A., Walia, V., Singh, S., Bajwa, B. S., Mahajan, S., Dhar, S., et al. (2012). Earthquake precursory studies at Amritsar Punjab, India using radon measurement techniques. *International Journal of Physical Sciences*, 7(42), 5669–5677.
- Mehra, R., & Bala, P. (2013). Estimation of annual effective dose due to radon level in indoor air and soil gas in Hamirpur district of Himachal Pradesh. *Journal of Geochemical Exploration*, 142, 16–20.
- Mujahid, S. A., Hussain, S., & Ramzan, M. (2010). Measurement of radon exhalation rate and soil gas radon concentration in areas of southern Punjab, Pakistan. *Radiation Protection Dosimetry*, 140, 300–303.
- Nero, A. V. (1988). Radon and its decay products in indoor air: an overview. In: W. W. Nazaroff & A. V. Nero Jr., (Eds.) *Radon and its decay products in indoor air* (pp. 1–53). New York: Wiley.
- Pascoe, E. H. (1964). *A manual of the Geology of India and Burma*, vol. I–IV, 3rd edn (pp. 1757–1811). Delhi: Government of India press.
- Prasad, Y., Prasad, G., Gusain, G. S., Choubey, V. M., & Ramola, R. C. (2008). Radon exhalation rate from soil samples of South Kumaun Lesser Himalayas, India. *Radiation Measurements*, 43, 369–374.
- Ramola, R. C., & Choubey, V. M. (2003). Measurement of radon exhalation rate from soil samples of Garhwal Himalaya, India. *Radioanalytical and Nuclear Chemistry*, 256, 219–223.
- Ranga, Rao A., Agarwal, R. P., Sharma, U. N., Bhalla, M. S., & Nanda, A. C. (1988). Magnetic polarity stratigraphy and vertebrate palaeontology of the Upper Siwalik Subgroup of Jammu Hills, India. *Geological Society of India*, 31, 361–385.
- Righi, S., & Bruzzi, L. (2006). Natural radioactivity and radon exhalation in building materials used in Italian dwellings. *Journal of Environmental Radioactivity*, 88, 158–170.

- Sahni, M. R., Mathur, L. P. (1964). Stratigraphy of the Siwalik Group. Inter-geology, Congo 22nd session.
- Sahoo, B. K., Nathwani, D., Eappen, K. P., Ramachandran, T. V., Gaware, J. J., & Mayya, Y. S. (2007). Estimation of radon emanation factor in Indian building materials. *Radiation Measurements*, 42, 1422–1425.
- Saini, K., & Bajwa, B. S. (2017). Mapping natural radioactivity of soil samples in different regions of Punjab, India. *Applied Radiation and Isotopes*. <https://doi.org/10.1016/j.apradiso.2017.05.013>.
- Sharma, S., Kumar, A., & Mehra, R. (2017). Variation of ambient gamma dose rate and indoor radon/thoron concentration in different villages of Udhampur district, Jammu and Kashmir, India. *Radiation Protection and Environment*, 40, 133–141.
- Sharma, S., Kumar, A., Mehra, R., Kaur, M., & Mishra, R. (2018). Assessment of progeny concentrations of $^{222}\text{Rn}/^{220}\text{Rn}$ and their related doses using deposition based progeny sensors. *Environmental Science and Pollution Research*, 25, 11440–11453.
- Singh, S., Sharma, D. K., Dhar, S., & Randhawa, S. S. (2006). Geological significance of soil gas radon: A case study of Nurpur area district Kangra, Himachal Pradesh, India. *Radiation Measurements*, 4, 482–485.
- Singh, J., Singh, H., Singh, S., & Bajwa, B. S. (2010). Measurement of soil gas radon and its correlation with indoor radon around some areas of Upper Siwaliks, India. *Journal of Radiological Protection*, 30, 63–71.
- Stoulos, S., Manolopoulou, M., & Papastefanou, C. (2003). Assessment of natural radiation exposure and radon exhalation from building materials in Greece. *Journal of Environmental Radioactivity*, 69, 225–240.
- Stranden, E. A., Kolstad, A. K., & Lind, B. (1984). Radon exhalation; moisture and temperature dependence. *Health Physics*, 47, 480.
- Tanner, A. B. (1964). Radon migration in the ground: A review. In J. A. S. Adams & W. M. Lowder (Eds.), *The natural radiation environment* (pp. 161–190). Chicago: Chicago University of Chicago press.
- Tareen, A. D. K., Rafique, M., Kearfott, K. J., Basharat, M., & Shafique, B. (2016). Soil gas radon mapping of Muzaffarabad city, Pakistan. *Nuclear Technology and Radiation Protection*, 3, 291–298.
- UNSCEAR. (1988). Sources and effects of ionizing radiation. United Nations Scientific Committee on the Effect of Atomic Radiation Annex A., United Nations, New York.
- UNSCEAR. (2008). *Sources and biological effects of ionizing radiation*. New York: United Nations.
- US Environmental Protection Agency. (2012). A citizens guide to radon: The guide to protecting yourself and your family from radon; EPA 402/K-12/002, www.epa.gov/radon.
- Walia, V., Virk, H. S., & Bajwa, B. S. (2006). Radon precursory signals for some earthquakes of magnitude > 5 occurred in N-W Himalaya. *Pure and Applied Geophysics*, 163, 711–721.

(Received March 15, 2018, revised July 2, 2018, accepted July 3, 2018, Published online July 13, 2018)